

# Dyon-Skyrmion Lumps

Y. Brihaye<sup>◊</sup>, B. Kleihaus<sup>†</sup> and D. H. Tchrakian<sup>†\*</sup>

<sup>◊</sup>Physique-Mathematique, Universite de Mons- Hainaut, Mons, Belgium

<sup>†</sup>Department of Mathematical Physics, National University of Ireland Maynooth,  
Maynooth, Ireland

<sup>\*</sup>School of Theoretical Physics – DIAS, 10 Burlington Road, Dublin 4, Ireland

## Abstract

We make a numerical study of the classical solutions of the combined system consisting of the Georgi-Glashow model and the  $SO(3)$  gauged Skyrme model. Both monopole-Skyrmion and dyon-Skyrmion solutions are found. A new bifurcation is shown to occur in the gauged Skyrme solution sector.

# 1 Introduction

There are two 3+1 dimensional  $SO(3)$  gauge field models which support static soliton solutions. One is the Georgi-Glashow (GG) model which supports the well known monopole [1], and the other is the  $SU(2)_{L+R}$ , or vector, gauged Skyrme model [2, 3] which also supports  $SO(3)$  gauged Skyrmions. In addition to the monopole, the GG model supports also dyon solutions [4] which in addition to the magnetic charge carry an electric charge as well. The topological stability of the monopole comes from the magnetic charge, which is descended from the second Chern-Pontryagin charge, while the topological charge of the gauged Skyrmion is the degree of the map.

Combining these two models, we have a new system whose topological charge is a sum of the respective charges, and it can reasonably be expected that this system also supports static finite energy solitons. Note that in this case the local  $SO(3)$  symmetry is broken down to  $U(1)$  via the Higgs mechanism, in contrast to the  $SO(3)$  gauged Skyrme model on its own, in which case the local  $SO(3)$  symmetry is not broken at all and 3 massless gauge bosons survive. In this preliminary investigation, this is precisely what we have done. Using numerical methods, we verify that such solutions exist. Moreover, we have sought and found both monopole-Skyrmion and dyon-Skyrmion solutions, and studied some of their properties. The combined system supports solutions also with zero monopole charge, unit Baryon charge, as well as with unit monopole charge, zero Baryon charge.

Even though this is a self contained numerical study of the classical solutions alluded to above, it is in order to put it into context both in the background of previous work involving the gauging of the Skyrme model [5], and, from the viewpoint of its potential physical relevance.

The Skyrme model was gauged by Witten in Ref. [6], and others e. g. in Refs. [7]. These works were carried out in the context of current algebra results, and were not concerned with the solitonic aspects of the gauged Skyrmion. That was done subsequently by many authors [14] where gauged Skyrme solitons were studied with the aim of explaining the low energy properties of Hadrons. Also in the context of electroweak theory, which can be regarded as a gauged Skyrme model in the limit of very high Higgs mass, Rubakov [9] and Eilam *et al.* [10] considered the static classical solutions of the  $SU_L$  gauged Skyrme model. In all these cases, there is no topological lower bound and the classical solutions are metastable, but for certain values of the parameters in one of these models [9, 10] a stable branch of solitons appears as a result of catastrophic behaviour. The advantage of the gauging used in Refs. [9, 10] is that the 4-divergence of the topological current does not vanish but equals the local chiral anomaly [11, 12], which can present itself as a mechanism for Baryon number violation as explained in Ref. [9].

In the context of Baryon number violation, there is an older mechanism suggested by Rubakov [13] and by Callan [14] where monopole-(left-handed massless) Fermion interactions lead to Fermion number nonconservation. The mechanism involves the fluctuations of the electric field, in the presence of the magnetic field of the monopole,

giving rise to nonzero chiral anomaly and hence Fermion number violation. This was shown for the case of massless (left-handed) Fermions, by scattering with the monopole, which describes a high energy process. The approximation techniques employed [14, 13] are neither perturbation theoretic nor semiclassical. To describe a low energy process such as a decay, it would be more appropriate to deal with a process that is susceptible to semiclassical analysis. To this end, Callan and Witten [15] replaced the massless Fermions by the Skyrme soliton [5], interacting with the (Abelian) magnetic field of the monopole. While they [15] did not seek to demonstrate the existence of a  $U(1)$  gauged Skyrme, this is implicit in their work and has recently been verified numerically [17]. In the background of this it is hoped that the present work, which sets out to find the monopole-Skyrmion and dyon-Skyrmion solutions, would be of concrete usefulness to a semiclassical method of describing Baryon number decay. In particular the dyon-Skyrmion excites a nonzero classical quantity for the chiral anomaly, which can lead to chirality breaking as pointed out long ago by Marciano and Pagels [16].

In Section 2 we present the model and give the topological lower bounds on the static energy. In Section 3 we give the static spherically symmetric fields and the field equations in the static limit. Sections 4 and 5 deal, respectively, with the results of the numerical analysis of the  $\mathbf{A}_0 = 0$  and  $\mathbf{A}_0 \neq 0$  cases. Section 5 in particular, includes an in depth analysis of the Julia-Zee dyon [4]. We summarise and discuss our results in Section 6.

## 2 The Model

The model under consideration is the combination of the Georgi-Glashow (GG) model and of the  $SO(3)$  gauged  $O(4)$  (Skyrme) model studied previously in Refs. [2, 3]. We state the Lagrangian of each of these models separately, defined in four dimensional Minkowski space, each being normalised properly so that the value of the energy of the static soliton in each case lies above its own topological lower bound. The static solutions in question satisfy the Euler- Lagrange equations of the static energy density functional, which is the static hamiltonian in the temporal gauge. In the GG case, this is the 'tHooft- Polyakov [1] monopole, while in the latter case it is the soliton studied in Refs. [2, 3].

The GG model is described by

$$\mathcal{L}_{GG} = -\frac{1}{4}\lambda_0^4|F_{\mu\nu}^\alpha|^2 + \frac{1}{2}\lambda_1^4|D_\mu\Phi^\alpha|^2 - \frac{1}{4}\lambda_2^4(\eta^2 - |\Phi^\alpha|^2)^2, \quad (1)$$

$$F_{\mu\nu}^\alpha = \partial_\mu A_\nu^\alpha - \partial_\nu A_\mu^\alpha + \varepsilon^{\alpha\beta\gamma} A_\mu^\beta A_\nu^\gamma, \quad D_\mu\Phi^\alpha = \partial_\mu\Phi^\alpha + \varepsilon^{\alpha\beta\gamma} A_\mu^\beta\Phi^\gamma. \quad (2)$$

The late Greek indices  $\mu, \nu, \dots$  label the Minkowski space vectors, while the early Greek indices  $\alpha, \beta, \dots = 1, 2, 3$  label the elements of the algebra of the gauge group  $SO(3)$ . The Latin letters  $a, b, \dots = 1, 2, 3, 4$ , so that  $a = (\alpha, 4)$  are reserved for the  $O(4)$  Skyrme model. In eq. (1) the constant  $\eta$  is the vacuum expectation value (VEV) of the Higgs

field and like the latter has the inverse dimension of a length. The constants  $\lambda_0, \lambda_1$  and  $\lambda_2$  are all dimensionless.

The  $SO(3)$  gauged Skyrme model is described by

$$\mathcal{L}_{O(4)} = -\frac{1}{4}\kappa_0^4|F_{\mu\nu}^\alpha|^2 + \frac{1}{2}\kappa_1^2|D_\mu\phi^a|^2 - \frac{1}{8}\kappa_2^4|D_{[\mu}\phi^a D_{\nu]}\phi^b|^2 \quad (3)$$

$$D_\mu\phi^\alpha = \partial_\mu\phi^\alpha + \varepsilon^{\alpha\beta\gamma}A_\mu^\beta\phi^\gamma, \quad D_\mu\phi^4 = \partial_\mu\phi^4. \quad (4)$$

The constants  $\kappa_0$  and  $\kappa_2$  are dimensionless and the constant  $\kappa_1$  has dimension of a inverse length. The reason we keep all the coupling constants arbitrary in eqs. (1) and (3) will appear soon.

When we consider the static Hamiltonians corresponding to the Lagrangians above in the temporal gauge, i. e.  $A_0 = 0$ , we can write the following topological identities:

$$\int d\mathbf{r} \mathcal{H}_{GG} \geq 4\pi\eta\lambda_0^2\lambda_1^2 M, \quad (5)$$

$$\mathcal{H}_{GG} = \frac{1}{4}\lambda_0^4|F_{jk}^\alpha|^2 + \frac{1}{2}\lambda_1^4|D_j\Phi^\alpha|^2 + \frac{1}{4}\lambda_2^4(\eta^2 - |\Phi^\alpha|^2)^2, \quad (6)$$

where the integer  $M$ , representing the index of the mapping  $\Phi^\alpha(\vec{x})$ , is the monopole topological charge. Similarly [3]

$$\int d\mathbf{r} \mathcal{H}_{O(4)} \geq 12\pi^2\kappa_1\kappa_2^2 \frac{1}{2\sqrt{1+9(\frac{\kappa_2}{\kappa_0})^4}} T \quad (7)$$

$$\mathcal{H}_{O(4)} = \frac{1}{4}\kappa_0^4|F_{jk}^\alpha|^2 + \frac{1}{2}\kappa_1^2|D_j\phi^a|^2 + \frac{1}{8}\kappa_2^4|D_{[j}\phi^a D_{k]}\phi^b|^2 \quad (8)$$

where the integer  $T$ , representing the index of the mapping  $\phi^a(\vec{x})$ , is the Skyrmion topological charge. In the Skyrme description of hadrons,  $T$  is identified with the baryon number.

In the following will consider also the equations resulting from the superposition of the two lagrangians eqs. (1) and (3)

$$\mathcal{L}_m = \mathcal{L}_{GG} + \mathcal{L}_{O(4)}. \quad (9)$$

The finite energy configurations of this mixed lagrangian are characterized by the couple of integers  $M, T$ . Classical solutions corresponding to the two different topological excitations can then be constructed, they correspond to the configuration with minimal energy in a class  $M, T$ .

In order to normalize the fields conventionally, we have to choose

$$\lambda_0^2 = \frac{1}{e} \cos(\theta), \quad \kappa_0^2 = \frac{1}{e} \sin(\theta), \quad \lambda_1^4 = 1 \quad (10)$$

where  $e$  denotes the gauge coupling constant. With the choice  $\theta = \pi/4$ , the topological inequality relating  $\mathcal{H}_m$  to the class of solutions of indexes  $M, T$  reads

$$\int d\mathbf{r} \mathcal{H}_m \geq \frac{4\pi\eta}{e} \left( \frac{1}{\sqrt{2}}M + \frac{3\pi}{2} \sqrt{\frac{\xi\kappa}{\sqrt{1+18\kappa}}} T \right) \quad (11)$$

where

$$\lambda = \frac{\lambda_2^4}{e^2} , \quad \xi = \frac{1}{\eta^2} \kappa_1^2 , \quad \kappa = e^2 \kappa_2^4. \quad (12)$$

In eq. (12),  $\lambda$  is defined for later convenience. Note that the topological lower bound eq. (11) can be refined by an optimal value of the mixing angle  $\theta$ , depending on the parameters  $\lambda_1, \lambda_2, \kappa_1, \kappa_2$ . To achieve this it is necessary to solve a complicated non linear equation, which we shall not pursue here.

### 3 Static spherically symmetric equations

The classical equations corresponding to eqs. (1), (3) and (9) are in general intractable. We will restrict our search of solutions to the static and spherically symmetric case. If we choose to employ the temporal gauge in the static limit, the Euler- Lagrange equations will reduce to the variational equations arising from the static Hamiltonians pertaining to the Lagrangians eqs. (1) and (3). The latter would be bounded from below by the monopole charge and the Baryon number densities, respectively. Hence the solutions to the classical equations of each of these static Hamiltonians, separately, can describe the 'tHooft-Polyakov monopole [1] and the soliton of the  $SO(3)$  gauged Skyrme model [2, 3]. The Euler-Lagrange equations of the Hamiltonian of the combined static system, i. e. GG-Skyrme, in the temporal gauge also supports soliton solutions since the Hamiltonian is again bounded from below by the two topological charges eq. (11). This is one of the problems studied in the present work yielding the monopole-Skyrmion solitons.

If instead of employing the temporal gauge we proceed like Julia and Zee [4] and solve the Euler-Lagrange equations pertaining to the Lagrangian eq. (9) defined on Minkowski space in the static limit, the resulting solutions of the GG-Skyrme system describe the dyon-Skyrmion. This is the other problem studied in this work. As in the case of the dyon [4] on its own, we shall restrict to the spherically symmetric solutions only <sup>1</sup>.

The spherically symmetric Ansatz employed is

$$A_i^\alpha = \frac{a(r) - 1}{r} \varepsilon_{i\alpha\beta} \hat{x}^\beta, \quad A_0^\alpha = \frac{g(r)}{r} \hat{x}^\alpha \quad (13)$$

$$\Phi^\alpha = \eta h(r) \hat{x}^\alpha \quad (14)$$

$$\phi^\alpha = \sin f(r) \hat{x}^\alpha, \quad \phi^4 = \cos f(r). \quad (15)$$

Notice that the functions  $a(r)$ ,  $h(r)$ ,  $g(r)$  and  $f(r)$  are dimensionless. We find it useful to introduce a dimensionless radial variable

$$x = M_W r , \quad M_W \equiv e\eta \quad (16)$$

---

<sup>1</sup>In this case the classical equations simplify sufficiently to become tractable. To our knowledge the only dyon solutions known are the spherically symmetric Julia-Zee[4] dyons.

Substituting the Ansätze eqs. (13)-(15) into the static limit of the Lagrangian eq. (9), leads to the following one dimensional (radial) Lagrangian density  $L_m$ , defined by

$$\int L_m dx = \int \mathcal{L}_m d\mathbf{r} = E_1 - E_2 \quad (17)$$

with

$$E_p \equiv \frac{4\pi}{e} \eta \tilde{E}_p = \frac{4\pi}{e} \eta \int dx \mathcal{E}_p \quad , \quad p = 1, 2 \quad (18)$$

$$\mathcal{E}_1 = \frac{1}{2} x^2 (g')^2 + a^2 g^2 \quad (19)$$

$$\begin{aligned} \mathcal{E}_2 = & (a')^2 + \frac{(a^2 - 1)^2}{2x^2} \\ & + \frac{1}{2} x^2 (h')^2 + a^2 h^2 + \frac{\lambda}{4} x^2 (h^2 - 1)^2 \\ & + \frac{\xi}{2} [x^2 (f')^2 + 2a^2 \sin^2 f] \\ & + \kappa a^2 \sin^2 f [(f')^2 + a^2 \frac{\sin^2 f}{2x^2}] \end{aligned} \quad (20)$$

where we have separated the contribution  $E_1$  due to the electric field and the prime denotes the derivative with respect to  $x$ .

The static classical equations corresponding to the Lagrangian density  $\mathcal{L}_m$ , in the spherically symmetric Ansatz, turn out to be equivalent to the equations obtained by varying the effective one dimensional density (see eqs. (19) and (20))  $\mathcal{E}_1 - \mathcal{E}_2$  with respect to the radial functions  $a, g, h$  and  $f$ . These equations are obtained straightforwardly and we do not list them here. We note however, that for each function the corresponding variational equation can be solved trivially by setting this function to zero.

It will be useful to present their asymptotic forms in the  $x \gg 1$  region, to facilitate subsequent explanations. They are, in order of the variations of  $a, g, h$  and  $f$  :

$$a'' = a \left( \frac{a^2 - 1}{x^2} + h^2 - g^2 + \xi \sin^2 f + \dots \right) \quad (21)$$

$$(x^2 g')' = 2g a^2 \quad (22)$$

$$(x^2 h')' = h(2a^2 + \lambda x^2 (h^2 - 1)) \quad (23)$$

$$(x^2 f')' = 2a^2 \sin f \cos f + o(\kappa/\xi). \quad (24)$$

Following [4], we define the energy of a configuration by  $E = E_1 + E_2$ , which coincides with the volume integral of the static Hamiltonian obtained in the usual way from the gauge invariant stress tensor. The topological lower bound for  $E_2$  follows immediately from eqs. (5), (7) and (11).

## 4 Numerical results, case $\mathbf{A}_0 = 0$

We first discuss the classical solutions in absence of the electric field, i. e. with  $g(x) = 0$ . Eq. (22) is trivially solved and we are left with a system of three non linear differential equations. Only the part  $E_2$  of the action is relevant in this case. In the following, we will conveniently denote the value  $\tilde{E}_2$  of the solution with given  $M$  and  $T$  by

$$E_{MT}(\lambda, \xi, \kappa). \quad (25)$$

We now describe the four cases with  $M \leq 1$  and  $T \leq 1$ .

### 4.1 Case $M = 0, T = 0$

This corresponds to the class of the vacuum which is not spherically symmetric. It has a zero energy

$$E_{00}(\lambda, \xi, \kappa) = 0. \quad (26)$$

### 4.2 Case $M = 1, T = 0$

This case corresponds to the celebrated SU(2) magnetic monopole [1]. Since  $T = 0$ , it has  $f(r) = 0$ ; as a consequence, the parameters  $\xi$  and  $\kappa$  are irrelevant for this case. The boundary conditions and asymptotic behaviour of the functions  $a, h$  read

$$a(0) = 1, \quad h(0) = 0 \quad (27)$$

$$a(x) \simeq Ae^{-x}, \quad h(x) \simeq 1 - Be^{-\sqrt{2\lambda}x} \quad (x \rightarrow \infty) \quad (28)$$

where  $A, B, F$  are constants. The values of the energy of the monopole solution were computed long ago [18] (our numerics fully reproduces these values); the energy increases monotonically with  $\lambda$  as demonstrated in Table 1.

In the Bogomol'nyi limit,  $\lambda = 0$ , the energy coincides with the topological lower bound, i. e. (omitting the parameters  $\xi$  and  $\kappa$ )

$$E_{10}(\lambda) \geq E_{10}(0) = 1. \quad (29)$$

The solution, the Prasad-Sommerfield monopole, is expressed in terms of elementary functions [19]. Its behaviour near the origin is given by (27) but, for  $x \rightarrow \infty$ , we have

$$a(x) \simeq xe^{-x}, \quad h(x) \simeq 1 - \frac{1}{x} \quad (30)$$

instead of (28).

### 4.3 Case $M = 0, T = 1$

In this case, there is no Higgs field and consequently no Higgs potential. Correspondingly, the topological lower bound reads

$$E_{01}(\lambda, \xi, \kappa) \geq \frac{3\pi}{2} \frac{\sqrt{\xi\kappa}}{\sqrt{1+9\kappa}} \quad (31)$$

independently of  $\lambda$ . The static equations describe the gauged Skyrmion studied in Ref. [3].

The parameter  $\xi$  can be changed by a rescaling of the radial variable  $x$ . Comparison of the energies of the gauged Skyrmion and of the monopole is demonstrated in Table 1 and Fig. 1. In Table 1 we list the energies for various values of  $\lambda$  for fixed  $\xi = 1$  and  $\kappa = 0.4$ , while in Fig. 1  $\kappa$  varies and we have fixed  $\lambda = \xi = 1$ .

Let us now come to the detailed discussion of the solutions in the region  $\kappa \approx 0.8$ . For completeness, it is useful to summarise the possible boundary conditions available for the gauged Skyrmion. At the origin  $x = 0$  the behaviour of the radial functions is uniquely determined by the condition of continuity of the fields at the origin:

$$a(x) = 1 + A_1 x^2 + o(x^3) \quad , \quad f(x) = \pi + F_1 x + o(x^2). \quad (32)$$

In contrast, in the  $x \gg 1$  asymptotic region, several conditions are consistent with the finiteness of the energy. Classical solutions of the equations have been obtained [3] with the two following sets

$$\text{Type A} : \quad a \approx 1 - \frac{A}{x} \quad , \quad f \approx \frac{F}{x^2} \quad (33)$$

$$\text{Type B} : \quad a \approx \frac{A}{x^\alpha} \quad , \quad f \approx \frac{F}{x} \quad (34)$$

where  $\alpha \equiv (\sqrt{4F^2 - 3} - 1)/2$ .

The following results were obtained in [3]. For small values of  $\kappa$ , the solution is of type A, its energy increases monotonically from  $E = 0$  (for  $\kappa = 0$ ) and the branch (say branch A) stops at a critical value  $\kappa = \kappa_A^{cr} \approx 0.8091$ . For large values of  $\kappa$  (in fact for  $\kappa > \kappa_B^{cr} \approx 0.69122$ ) the solution is of type B. We call this branch B. By using arguments of catastrophe theory [10], one can reasonably expect the occurrence of a third branch of solutions on the interval  $\kappa \in [\kappa_B^{cr}, \kappa_A^{cr}]$ , as was explained in [3].

A third branch indeed exists. The solutions on this branch obey the condition of type A and therefore we refer to it as branch  $\tilde{A}$ . The energies of the three branches of solutions are depicted on Fig. 2. The branches A and  $\tilde{A}$  terminate at  $\kappa = \kappa_A^{cr}$ , forming a cusp catastrophe. The transitions of the profile of the solutions from branch A to branch  $\tilde{A}$  is smooth.

In contrast, when the limit  $\kappa \rightarrow \kappa_B^{cr}$  is considered, the solutions of the branch  $\tilde{A}$  approach the limit of branch B in a subtle way. For instance, the value  $x_m$  for which the function  $a(x)$  has a minimum (say  $a_m$ ) tends to infinity, while  $a_m$  tends to zero. For values of  $\kappa$  close to  $\kappa_1$ , the solutions of branches  $\tilde{A}$  and B coincide on a large

interval of  $x$  (typically on  $x \in [0, 10^7]$  for  $\kappa = 0.6914$ ) and deviate from each other for larger values of  $x$ . In the limit  $\kappa \rightarrow \kappa_B^{cr}$  this interval becomes infinitely large and the two solutions deviate at infinity. This can clearly be seen from Fig. 3. A similar demonstration can be made for the function  $f(x)$ , namely that near the critical point  $\kappa_B^{cr}$  these functions for the two solutions on branches  $B$  and  $\tilde{A}$  also coincide. We do not display the graphs analogous to Fig. 3 in this case. The behaviour of the solutions is further illustrated by Figs. 4 and 5 where we plot respectively the value of  $F_1$  (defined in eq. (32)) for the three branches and the value of  $\alpha$  as a function of  $\kappa$ .

Fig. 2 furnishes a simple interpretation of the three solutions. To discuss it, we introduce  $\kappa_{AB}^{cr}$  as the value of  $\kappa$  where the energy of the branches  $A$  and  $B$  coincide ( $\kappa_{AB}^{cr} \approx 0.785$ ). On the interval  $\kappa \in [\kappa_B^{cr}, \kappa_{AB}^{cr}]$  the solution on branch  $A$  constitutes the absolute minimum of the energy functional  $E_2$ , while the one on branch  $B$  is a local minimum. The solution on the branch  $\tilde{A}$  is a sphaleron corresponding to a saddle point which represents the energy barrier between the two minima. The situation is similar on the interval  $\kappa \in [\kappa_{AB}^{cr}, \kappa_A^{cr}]$ ; the absolute (resp. local) minimum energy configuration is then on branch  $B$  (resp.  $A$ ). As  $\kappa$  approaches the critical value  $\kappa_B^{cr}$  the local minimum of branch  $B$  approaches the saddle point of branch  $\tilde{A}$ . At the critical  $\kappa$  both coincide and form an inflection point. For  $\kappa < \kappa_B^{cr}$  this point is no longer an extremum and the solutions of branches  $B$  and  $\tilde{A}$  cease to exist. The global minimum of branch  $A$  is then the only extremum and only branch  $A$  solutions exist. The same scenario applies at the other critical value  $\kappa_A^{cr}$  where the solutions of branches  $A$  and  $\tilde{A}$  stop to exist and only branch  $B$  solutions exist.

#### 4.4 Case $M = 1, T = 1$

It is natural to call this solution the "monopole-Skyrmion". The three functions  $a, h, f$  are non trivial and obey the following boundary conditions at  $x = 0$  and as  $x \rightarrow \infty$ , respectively,

$$a(0) = 1 \quad , \quad h(0) = 0 \quad , \quad f(0) = \pi \quad (35)$$

$$a(x) \simeq Ae^{-x} \quad , \quad h(x) \simeq 1 - Be^{-\sqrt{2\lambda}x} \quad , \quad f(x) \simeq \frac{F}{x} \quad (36)$$

where  $A, B$  and  $F$  are constants. In contrast to the case of the gauged Skyrmion solution [3], the finite energy condition leads to a unique asymptotic behaviour of the solution.

The energy of the solution is given in Table 1 for several values of  $\lambda$  (for  $\xi = 1$  and  $\kappa = 0.4$ ), indicating that the energy of the monopole-Skyrmion varies rather slightly with  $\lambda$ . The corresponding lower bound inequality reads

$$E_{11}(\lambda, \xi, \kappa) \geq \frac{1}{\sqrt{2}} + \frac{3\pi}{2} \frac{\sqrt{\xi\kappa}}{\sqrt{1+18\kappa}}. \quad (37)$$

## 4.5 General properties

We have constructed numerically the three non trivial topological solitons above for numerous values of the coupling constants  $\lambda, \xi, \kappa$  and computed their energies. In order to give an idea of the relative magnitudes for the different classes, let us choose  $\lambda = 1, \xi = 1, \kappa = 0.4$ , then

$$E_{00} = 0 \quad , \quad E_{10} \approx 1.29 \quad , \quad E_{01} \approx 2.98 \quad , \quad E_{11} \approx 3.53 \quad . \quad (38)$$

The Bogomol'nyi limit  $\lambda = 0$  is of particular interest since in that case the monopole saturates its topological lower bound. Choosing again  $\xi = 1, \kappa = 0.4$ , we find

$$E_{00} = 0 \quad , \quad E_{10} = 1.0 \quad , \quad E_{01} \approx 2.98 \quad , \quad E_{11} \approx 3.45 \quad (39)$$

The behaviour of the solutions in the limit  $\kappa \rightarrow 0$ , with  $\lambda, \xi$  fixed, was carefully analysed. Our numerical analysis strongly supports the following formula :

$$\lim_{\kappa \rightarrow 0} E_{M1}(\lambda, \xi, \kappa) = E_{M0}(\lambda, \xi, 0) \quad , \quad \text{for } M = 0, 1 \quad (40)$$

as illustrated by Fig. 1. Indeed, in the limit  $\kappa \rightarrow 0$ , the functions  $a(r), h(r)$  representing the solutions of the  $M = T = 1$  sector approach the profile of the monopole solution (i. e.  $M = 1, T = 0$ ). At the same time, the function  $f(r)$  is more and more peaked at  $r = 0$  (in particular  $\lim_{\kappa \rightarrow 0} f'(0) = \infty$ ) and tends to zero if  $r \neq 0$ .

This result demonstrates in particular that the coupling of the Skyrmion to a monopole cannot stabilise the Skyrmion; the Skyrme term is necessary to guarantee a localized structure to the  $T = 1$  soliton.

The same phenomenon occurs with the branch of the gauged Skyrmion ( $M = 0, T = 1$ ) [3]. The energy in this limit tends to zero, namely to the energy of the vacuum ( $M = T = 0$ ).

A remark should be made concerning the interpretation of the monopole-Skyrmion as a bound system of a monopole with magnetic charge  $M$  and a gauged Skyrmion with baryon number  $T$ . Consider a monopole located in a region  $U_m$  centered at a point  $x_m$  and a gauged Skyrmion located in a region  $U_{Sk}$  centered at a point  $x_{Sk}$  far away from each other. Then the Skyrmion field and the corresponding gauge field will vanish outside the region  $U_{Sk}$ . Consequently,  $U_m$  contains a pure monopole, consisting of a gauge field and a Higgs field. Outside  $U_m$  the gauge field will vanish, however, the Higgs field does not vanish. Instead it will be equal to its VEV  $\langle \Phi \rangle_{vac}$ . In the region  $U_{Sk}$  containing the Skyrmion the non-zero Higgs field is still present and we have to allow for interaction with the gauge field,  $|D_j \langle \Phi \rangle_{vac}^\alpha|^2$ . The Higgs vacuum is a constant far away from the monopole and generates masses for the gauge fields. Furthermore, the Higgs vacuum breaks the rotational symmetry. Consequently, the gauged Skyrmion solutions in the presence of a constant Higgs field will no longer possess spherical symmetry. In addition, it might be expected that the electro-magnetic flux will not vanish. If we impose the condition for the Higgs vacuum that the interaction with the gauge field has to vanish,  $D_j \langle \Phi \rangle_{vac}^\alpha = \epsilon^{\alpha\beta\gamma} A_j^\beta \langle \Phi \rangle_{vac}^\gamma = 0$ , then we will

find that the gauge field has to be parallel to the Higgs vacuum in isospace. This also breaks the spherical symmetry.

To conclude, the interpretation of the monopole-Skyrmions as a bound state of a spherically symmetric monopole and a spherically symmetric gauged Skyrmion seems to be misleading.

## 5 Numerical results, case $\mathbf{A}_0 \neq 0$

In order to obtain a non trivial function  $g(x)$  from eq. (22), a non vanishing asymptotic value, say  $q$ , for this function has to be imposed [4]. In the asymptotic region  $x \gg 1$  eq. (22) is satisfied by

$$g(x) = q - \frac{c_1}{x} + \mathcal{O}(x^{-2}) \quad (41)$$

where  $q, c_1$  are constants and  $q$  plays a major role in the construction. The equations, together with the finite energy condition require  $0 \leq q \leq 1$ , which can be seen as follows. In eq. (21) the Higgs field and the dyon field contributions,  $h^2(x) - g^2(x)$ , generate asymptotically the mass term  $m_{(a)}^2 = 1 - q^2$  for the gauge field function  $a(x)$ . For  $q > 1$ ,  $m_{(a)}^2$  becomes negative and leads to an oscillating function  $a(x)$  in the asymptotic region. Consequently, the term  $a^2 g^2$  in eq. (17) is not integrable and no dyon solution exists for  $q > 1$ .

The electric charge, as defined in [4], is directly related to the constant  $c_1$  :

$$Q = \frac{1}{4\pi\eta} \int \vec{\Phi} \cdot \vec{F}_{0i} dS_i \equiv \frac{1}{e} \tilde{Q} \quad (42)$$

$$= \frac{1}{4\pi} \int (r^2 \frac{dg}{dr})|_{r \rightarrow \infty} \sin \theta d\theta d\phi = \frac{1}{e} c_1, \quad (43)$$

having used the Ansatz (13)-(14) and eq. (41).

Another very interesting quantity is the chiral anomaly due to the dyon-Skyrmion soliton whose classical solutions will be studied numerically. The anomaly equation for the chiral charge is

$$\begin{aligned} \frac{dQ_5}{dt} &= \frac{e^2}{8\pi^2} \int d\mathbf{x} \mathbf{E}_i \cdot \mathbf{B}_i \\ &= -\frac{e^2}{8\pi^2} 4\pi [g(r)(a(r) - 1)]_{r=0}^{\infty} = \frac{e^2}{2\pi} q, \end{aligned} \quad (44)$$

having used the Ansatz (13)-(14) and, eq. (41). We now discuss the solutions by adopting the same presentation as in the previous Section.

### 5.1 Case $M = 1, T = 0$

The solutions are the dyons of Julia and Zee [4]. Here we present an in depth analysis of this solution. The limit  $\lambda = 0$  corresponds to the Prasad-Sommerfield dyon [19]

(PS dyon). It is worth analysing this case separately because the solution can be computed analytically and it provides a good check of our numerical routines.

### Case $\lambda = 0$

The profile of the radial functions of the PS dyon reads [19]

$$a(x) = \frac{cx}{\sinh(cx)} \quad (45)$$

$$g(x) = \frac{cq}{\sqrt{1-q^2}} \left( \coth cx - \frac{1}{cx} \right) \quad (46)$$

$$h(x) = \frac{c}{\sqrt{1-q^2}} \left( \coth cx - \frac{1}{cx} \right) \quad (47)$$

and the PS monopole is recovered for  $q = 0$ . Our parameter  $q$  is related to  $\gamma$  of Ref. [19], by  $q = \tanh(\gamma)$ . We have chosen the arbitrary scale in the PS solution  $c = \sqrt{1-q^2}$  so that the asymptotic value of the Higgs field function  $h(x)$  of the PS solution given above be equal to 1, since we are also studying the dyons for the  $\lambda > 0$  case where the asymptotic value of  $h(x)$  equals 1. The charge and energy of the PS dyon are given by

$$\tilde{Q} = \frac{q}{\sqrt{1-q^2}} , \quad \tilde{E} = \frac{1}{\sqrt{1-q^2}} \quad (48)$$

$$\tilde{E}_1 = \frac{q^2}{2\sqrt{1-q^2}} , \quad \tilde{E}_2 = \left(1 - \frac{1}{2}q^2\right) \frac{1}{\sqrt{1-q^2}} \approx 1 + \frac{1}{8}q^4 + o(q^{-6}) \quad (49)$$

For small values of  $q$  the "magnetic" contribution to the energy,  $E_2$ , varies slightly with  $q$ , accounting for the feed back of the electric charge on the classical magnetic energy. We would like to stress that our numerical results are in full agreement with these exact formulas.

The dependence of the charge  $\tilde{Q}$  of the PS dyon as a function of  $q$  is represented in Fig. 6 (curve *a*). Similarly we have reported on Fig. 7 (curve *a*) the energy  $\tilde{E}$  of the PS dyon as a function of  $\tilde{Q}$ . Clearly the energy and the charge of the PS dyon can be arbitrarily large when  $q \rightarrow 1$ .

### Case $\lambda \neq 0$

For the dyon solution, the boundary conditions for the function  $g(x)$  can be read from eq. (41), and those of the functions  $a(x)$ ,  $h(x)$  from eqs. (27) and (28), with the exception of the behaviour of the function  $a(x)$  in the  $x \gg 1$  region, which now takes the form

$$a(x) \simeq Ae^{-\sqrt{1-q^2}x} . \quad (50)$$

The main distinguishing feature of the  $\lambda \neq 0$  dyon vs. the PS dyon is that its electric charge and its classical energy are bounded for  $q \in [0, 1]$ .

This phenomenon appears clearly in Fig. 6 and Fig. 7 respectively, where the quantities  $\tilde{Q}$  as a function of  $q$ , and  $\tilde{E}$  as a function of  $\tilde{Q}$ , are plotted for  $\lambda = 0.5$ .

More generally, it appears that the electric charge of the dyon constructed with a given value of the parameter  $q$  decreases when  $\lambda$  increases. The three bullets on Fig. 7 represent the data given in [4]; according to our numerical results they should lie on line  $b$ . Our numerical results therefore slightly disagree with [4].

The star on line  $b$  of Fig. 7 indicates the maximal accessible charge of the dyon solutions for a fixed value of  $\lambda$ . This contrasts with line  $a$  which asymptotically tends to infinity, in agreement with eqs. (48) and (49). The solutions with maximal electric charge and energy correspond to the case  $q = 1$  which we discuss next.

### Case $q = 1$

In the limit  $q = 1$  in eq. (41) the equation (21) ceases to impose the exponential decay eq. (50) for the function  $a(x)$ ; we have instead

$$a(x) \simeq Ae^{-\sqrt{8c_1}x} \quad \text{for } x \rightarrow \infty \quad (51)$$

where  $c_1$  is defined in eq. (41).

Fixing  $\lambda \neq 0$ , the electric charge (and similarly the classical energy) of the dyon cannot exceed a critical value, say  $Q_{cr}(\lambda)$ . This quantity is plotted against  $\lambda$  on Fig. 8 (solid line).

### 5.2 Case $M = 0, T = 1$

No finite energy dyon-like solutions supporting a non-vanishing (non-Abelian) electric field can be found in this case. Due to the absence of the Higgs field ( $h = 0$ ), eq. (21) leads to an oscillating asymptotic behaviour of  $a(x)$ . The term  $a^2g^2$  in the energy eq. (17) can therefore not be integrated.

### 5.3 Case $M = 1, T = 1$

The boundary conditions compatible with a finite energy solution in this case are identical to eqs. (35), (36) and (41). It is possible to construct the dyon-Skyrmion solutions. The dyon-Skyrmion display many features of the dyons, discussed at length above. These features are illustrated by Figs. 6 and 7 (dashed curves  $c, d$  and  $e$ ) and by Fig. 8 (dashed line). In addition we illustrate the dependence of the energy on the Skyrme coupling constant  $\kappa$  in Fig. 9 (solid line) for  $q = 0.5$  and  $\lambda = 0$ . The energy is an increasing function of  $\kappa$ . In the limit of vanishing  $\kappa$  the energy of the dyon-Skyrmion converges to the energy of the dyon-monopole. This can be compared with the behaviour of the energy of the monopole-Skyrmion, shown (for  $\lambda = 1$ ) in Fig. 1, where for vanishing  $\kappa$  the energy tends to the energy of the monopole. For our considerations leading to our conclusions in Fig. 9, we have chosen  $q = 0.5$  as a typical value in the allowed range  $0 \leq q \leq 1$ . We expect that our results, summarised by the solid curve in Fig. 9, is typical for any allowed value of  $q$ , and also for any value of the Higgs coupling constant  $\lambda$ , except in the important case of

$\lambda = 0$  and  $q = 1$ . The dyon-Skyrmion characterised by the boundary value  $q = 1$  in the  $\lambda = 0$  model has peculiar and interesting properties which we analyse in the next paragraphs.

For  $\lambda = 0$  the solutions of eqs. (22) and (23) are proportional to each other. Assuming that  $h = 1$  at infinity, the proportionality constant is given by  $q$ , eq. (41). Thus for  $q = 1$  the functions  $h(r)$  and  $g(r)$  are identical. In this special case  $h^2(r)$  and  $g^2(r)$  cancel each other in eq. (21). Consequently, eqs. (21) and (24) reduce to the field equation of the gauged Skyrme model (Sec. 4.3), and can be solved independently of  $h(r)$ ,  $g(r)$ .

The solutions of these equations are now given by the branch B solutions of the gauged Skyrme model. Once a solution for the function  $a(r)$  is found the equations for the functions  $h(r)$  and  $g(r)$  can be solved. Recalling that the branch B solutions exist for all  $\kappa \geq \kappa_B^{cr}$ , we expect the existence of the dyon-Skyrmion solution for the same range of coupling constants  $\kappa$ . However, not all of these solutions are finite energy solutions. This can be seen easily by inspecting the static Hamiltonian  $\mathcal{E} = \mathcal{E}_1 + \mathcal{E}_2$  given in eqs. (19) and (20), where the contributions from the functions  $h(r)$  and  $g(r)$  do not cancel. The asymptotic behaviour of these terms is dominated by  $a^2(r)h^2(r)$ ,  $a^2(r)g^2(r)$ . Using the boundary conditions  $h(\infty) = 1$ ,  $g(\infty) = 1$  and the asymptotic form of the function  $a(r)$ , eq. (34), these terms behave like  $\approx A^2(\kappa)/x^{2\alpha(\kappa)}$  for large  $x$ , where  $\alpha(\kappa)$  is a function determined numerically. Thus the integration of these terms will give finite contributions only if  $\alpha(\kappa) > 1/2$ . This restricts the range of the coupling constant  $\kappa$  to  $\kappa_{1/2}^{cr} < \kappa < \infty$ , where  $\kappa_{1/2}^{cr}$  is defined by  $\alpha(\kappa_{1/2}^{cr}) = 1/2$ . For  $\xi = 1$  we find  $\kappa_{1/2}^{cr} = 0.7652$ .

In Fig. 9 we show the dependence of the energy on the coupling constant  $\kappa$  for  $q = 1$  (dotted line) and for  $q = 0.5$  (solid line). (For  $q < 1$ , as stated above, solutions exist for all values of  $\kappa$ , the energy is a monotonic function of  $\kappa$ , and the limit  $\kappa \rightarrow 0$  the energy approaches the energy of the dyon solution.) For  $q = 1$  the energy is an increasing function of  $\kappa$  for large values of  $\kappa$  only. It has a minimum at  $\kappa = 1.21$ . As  $\kappa$  approaches its critical value  $\kappa_{1/2}^{cr}$  the energy becomes increasingly large and diverges at  $\kappa = \kappa_{1/2}^{cr}$ .

The charge  $\tilde{Q}$  of the solutions is determined by the asymptotic behavior of the function  $g(r)$ , eq. (43). Solving the equation (22) for large  $x$  we find the following expressions for the charge

$$\tilde{Q} = \begin{cases} \lim_{x \rightarrow \infty} \left( c_1 - \frac{2A^2}{2\alpha - 1} x^{-(2\alpha-1)} \right) & \text{for } \alpha > \frac{1}{2}, \\ \lim_{x \rightarrow \infty} (2A^2 \ln(x)) & \text{for } \alpha = \frac{1}{2}, \\ \lim_{x \rightarrow \infty} \left( -\frac{2A^2}{2\alpha - 1} x^{-(2\alpha-1)} \right) & \text{for } \alpha < \frac{1}{2}. \end{cases} \quad (52)$$

Thus solutions with finite charge exist only for  $\alpha > 1/2$ , i. e. for the same range of the coupling constant  $\kappa$  where finite energy solutions exist.

In Fig. 6 we show the dependence of the charge on the parameter  $q$  for  $\kappa = 0.4$  and  $\kappa = 1.0$ . For  $\kappa = 0.4$  ( $< \kappa_{1/2}^{cr}$ ) there is no finite charge solution for  $q = 1$ .

Consequently, the charge as a function of  $q$  diverges as  $q$  approaches the value 1. In contrast, for  $\kappa = 1$  ( $> \kappa_{1/2}^{cr}$ ) the solution with  $q = 1$  exists and the charge is finite for all values of  $q \in [0, 1]$ .

In Fig. 7 the energy as a function of the charge is shown for  $\kappa = 0.4$  and  $\kappa = 1.0$ . For  $\kappa = 0.4$  ( $< \kappa_{1/2}^{cr}$ ) the energy and the charge can take arbitrarily large values. In this case the energy is a monotonically increasing function of the charge with no end point. For  $\kappa = 1$  ( $> \kappa_{1/2}^{cr}$ ) the energy is again a monotonically increasing function of the charge. However, only finite energy and charge solutions exist for this value of  $\kappa$ . Thus the graph of the function  $\tilde{E}(\tilde{Q})$  ends at the maximal value of the charge.

## 6 Summary and Discussion

We have found monopole-Skyrmion and dyon-Skyrmion solutions to an  $SO(3)$  gauged Higgs and  $O(4)$  sigma (Skyrme) model, in which both scalar matter fields interact with the gauge field but not with each other. The Higgs field is isovector, like in the GG model, while the  $S^3$  valued (sigma) field is gauged according to the prescription used in Refs. [2, 3].

In the  $A_0^\alpha = 0$  gauge the static Hamiltonian is bounded from below by the sum of the two topological charge densities, the monopole charge and the degree of the map of the  $S^3$  field on  $\mathbb{R}_3$ . Thus the imposition of spherical symmetry reduces the system to an one dimensional subsystem, and the resulting differential equations are integrated analytically in the asymptotic regions and then numerically. This yielded the monopole-Skyrmion.

In the  $A_0^\alpha \neq 0$  gauge, the Euler-Lagrange equations arising from the variation of the static Hamiltonian density do not yield a soliton with non-vanishing  $A_0^\alpha$  and hence have  $E_0^\alpha = 0$ . Instead, the variational equations arising from the (non positive-definite) Lagrangian density in the static limit support spherically symmetric solutions with  $E_i^\alpha \neq 0$ . This is also what happens with the JZ dyon. There [4], inspite of the non-positive-definiteness of the functional subjected to the variational principle, it happens that after taking the static limit and imposing spherical symmetry, these equations reduce to a set of consistent, i. e. not overdetermined, set of coupled ordinary differential equations. Their solutions support a non-vanishing  $A_0^\alpha$  field. These ordinary differential equations also result from the variation of a certain one-dimensional (radial) functional which, in contrast to the one dimensional energy functional, is not positiv definite.

In the light of the surprisingly successful outcome for the JZ dyon, we were motivated to address the same question for the  $SO(3)$  gauged  $O(4)$  model [2, 3]. Subjecting the Lagrangian to the variational principle and then taking the static limit and imposing spherical symmetry, we found that this also led to a consistent set of coupled ordinary differential equations. The same situation obtains with the composite model of this paper, and it is the dyon like soltions of these last equations which yielded the dyon-Skyrmion. Concerning the  $SO(3)$  gauged Skyrme model on its own, while its equations of motion reduce to a consistent set of coupled ordinary differential

equations, their solutions support only vanishing electric field.

As a byproduct of our study of the dyon-Skyrmion, we made a detailed re-analysis of the JZ dyon refining our understanding of the latter, for example exploring the dependence of the energy of the dyon on its electric charge.

An important result of the numerical analysis of the monopole-Skyrmion solution is that, as the coupling strength of the Skyrme term is shrunk down to zero the monopole-Skyrmion reduces to the monopole, as depicted in Fig. 1. Thus the monopole does not stabilise the  $SO(3)$  gauged sigma model without a Skyrme term, something that is not prohibited by the Derrick scaling requirement.

Perhaps the most interesting aspect of the dyon-Skyrmion occurs for the model in the PS limit ( $\lambda = 0$ ) in the special case where the boundary value  $q$  of the function  $g(r)$  parametrising  $A_0^\alpha$  equals 1. In this case, the equations governing the functions  $a(r)$  (parametrising the gauge field) and the function  $f(r)$  (governing the Skyrme field) decouple from the fields  $h(r)$  (parametrising the Higgs field) and  $g(r)$ . As a consequence the solutions for the functions  $a(r)$  and  $f(r)$  are just the (branch B of the) gauged-Skyrmion solutions and exist only for values of the Skyrme coupling constant larger than a critical value  $\kappa_B^{cr}$ , as seen from Fig. 2. However, when the integrations of the Higgs field function  $h(r)$  and of the dyon function  $g(r)$  are taken into account, then finite energy solution only exist if the Skyrme coupling constant is larger than the critical value  $\kappa_{1/2}^{cr} > \kappa_B^{cr}$ , see Fig. 9. The energy of the solution at this critical value is found to become infinite and for lower values of the Skyrme coupling constant no finite energy solution exists. The time rate of change of the chiral charge eq. (44) is equal to the integer 1 (up to normalisation) for all values of the Skyrme coupling constant  $\kappa$  down to the critical value  $\kappa_{1/2}^{cr}$ , below which no finite energy solutions exist. We hope that this result may prove relevant to the semiclassical description of monopole catalysis of Fermion number non-conservation. If for example it could be argued that the dyon-Skyrmion favoured by Nature is the solution to the system eq. (9) in the PS limit, with the asymptotic constant  $q = 1$ , i. e. for which the quantity  $\frac{dQ_5}{dt}$  is an integer (up to normalisation), then it would follow that below the critical value  $\kappa_{1/2}^{cr}$  there will be no  $Q_5$  violating rate. We intend to return to this question in the near future.

**Acknowledgements** We are greatful to V. A. Rubakov for helpful discussions. B. K. was supported by Forbairt grant SC/97-636, and Y.B. and D. H. T. acknowledge partial support from Forbairt project IC/97/019.

## References

- [1] G.'tHooft, Nucl. Phys. **B 79** (1974) 276; A.M. Polyakov, JETP Lett. **20** (1974) 194.
- [2] K. Arthur and D.H. Tchrakian, Phys. Lett. **B 378** (1996) 187.
- [3] Y. Brihaye and D. H. Tchrakian, Solitons/Instantons in d-dimensional  $SO(d)$  gauged  $O(d+1)$  dimensional Skyrme models. Mons Preprint, June 1997.

- [4] B. Julia and A. Zee, Phys. Rev. **D 11** (1975) 2227.
- [5] T.H.R. Skyrme, Proc. Roy. Soc.**A260** (1961) 127; Nucl.Phys. 31 (1962) 556.
- [6] E. Witten, Nucl. Phys. **B 223** (1983) 422.
- [7] O. Kaymakcalan, S. Rajeev and J. Schechter, Phys. Rev. **D 30** (1984), 2354, 434; Y. Brihaye, N.K. Pak and P. Rossi, Phys. Lett. **B 149** (1984) 191; Nucl. Phys. **254** (1985) 71.
- [8] see for example M. Chemtob, Nucl. Phys. **A 466** (1987) 509.
- [9] V.A. Rubakov, Nucl. Phys. **256** (1985) 509; J. Ambjorn and V.A. Rubakov, *ibid.* **B 256** (1985) 594.
- [10] G. Eilam, D. Klabucar and A. Stern, Phys. Rev. Lett. **56** (1986) 1331.
- [11] J. Goldstone and F. Wilczek, Phys. Rev. Lett. **47** (1981) 986.
- [12] E. D'Hoker and E. Farhi, Nucl. Phys. **B241** (1984) 109.
- [13] V.A. Rubakov, JETP Lett **33** (1981) 658; "Theta-vacua, massless fermions and non-abelian magnetic monopoles", in: Problems of High Energy Physics and Quantum Field Theory. Proc. 4th Int. Seminar, Protvino, 1981. IHEP, vol. 1, p.148-155; Nucl. Phys. **B 203** (1982) 311.
- [14] C.G. Callan, Phys. Rev. **25** (1982) 2141; *ibid.* **D 26** (1982) 2058.
- [15] C.G. Callan and E. Witten, Nucl. Phys. **B 239** (1985) 161.
- [16] H. Pagels, Phys Rev. **D13** (1976) 343; W. Marciano and H. Pagels, *ibid.* **D 14** (1976) 531.
- [17] B.M.A.G. Piette and D.H. Tchrakian, Topologically stable soliton in the  $U(1)$  gauged Skyrme model, hep-th/9709189
- [18] E.B. Bogomol'nyi and M.S. Marinov. Sov. J. Nucl. Phys. **23** (1976) 355.
- [19] M. K. Prasad and C. M. Sommerfield, Phys. Rev. Lett.**35** (1975) 760.

$\lambda$	monopole	monopole-Skyrmion ( $\xi = 1, \kappa = 0.4$ )	gauged Skyrmion ( $\xi = 1, \kappa = 0.4$ )
0.0	1.000	3.450	2.98
0.05	1.106	3.470	2.98
0.10	1.138	3.480	2.98
0.20	1.180	3.490	2.98
0.40	1.220	3.510	2.98
0.60	1.250	3.520	2.98
0.80	1.270	3.530	2.98
1.00	1.290	3.536	2.98

**Table 1**

The energies of the monopole, the monopole-Skyrmion and the gauged Skyrmion for several values of the Higgs coupling constant  $\lambda$ .

## Figure Captions

Figure 1 The energies eq. (25) of the monopole (line *a*), of the gauged Skyrmion (line *b*) and of the monopole-Skyrmion (line *c*) as functions of  $\kappa$  ( $\lambda = 1, \xi = 1$ ).

Figure 2 The energy of the gauged Skyrmion as a function of  $\kappa$  in the region of the phase transition. The branches  $A, \tilde{A}$  are represented by the solid line and branch  $B$  by the dashed line.

Figure 3 The (logarithm of the) function  $a(x)$  on the two branches  $B$  and  $\tilde{A}$  on a logarithmic scale for several values of  $\kappa$  approaching the critical value  $\kappa_B^{cr}$ .

Figure 4 The quantity  $F_1$  defined in eq. (32) is plotted as a function of  $\kappa$  for the branches  $A, \tilde{A}$  (solid line) and for the branch  $B$  (dashed line).

Figure 5 The quantities  $\ln(F - 1)$  and  $\ln(\alpha)$  (defined in eq. (34)) are plotted as functions of the parameter  $\ln(\kappa - \kappa_B^{cr})$ .

Figure 6 The values of the electric charge  $\tilde{Q}$  as a function of the parameter  $q$ . The solid lines represent the dyon for  $\lambda = 0$  (line *a*) and  $\lambda = 0.5$  (line *b*). The dashed lines represent the dyon-Skyrmion ( $\xi = 1$ ) for  $\lambda = 0, \kappa = 0.4$  (line *c*),  $\lambda = 0.5, \kappa = 0.4$  (line *d*) and  $\lambda = 0, \kappa = 1$  (line *e*).

Figure 7 The values of the energy  $\tilde{E}$  as a function of the parameter  $\tilde{Q}$ . The solid lines represent the dyon for  $\lambda = 0$  (line *a*) and  $\lambda = 0.5$  (line *b*). The dashed lines represent the dyon-Skyrmion ( $\xi = 1$ ) for  $\lambda = 0, \kappa = 0.4$  (line *c*),  $\lambda = 0.5, \kappa = 0.4$  (line *d*) and  $\lambda = 0, \kappa = 1$  (line *e*). The stars depict the points where the solution has maximal finite charge. The bullets correspond to the data of [4].

Figure 8 The value of the critical charge  $Q_{cr}$  as a function of  $\lambda$ . The solid line refers to the dyon solution. The dashed line refers to the dyon-Skyrmion solution for  $\xi = 1$  and  $\kappa = 0.4$ .

Figure 9 The energies of the dyon-Skyrmions with  $q = 1$  (solid line) and  $q = 0.5$  (dashed line) as functions of  $\kappa$  ( $\lambda = 0, \xi = 1$ ). The vertical dotted line indicates the critical value of  $\kappa$ .

Fig. 1

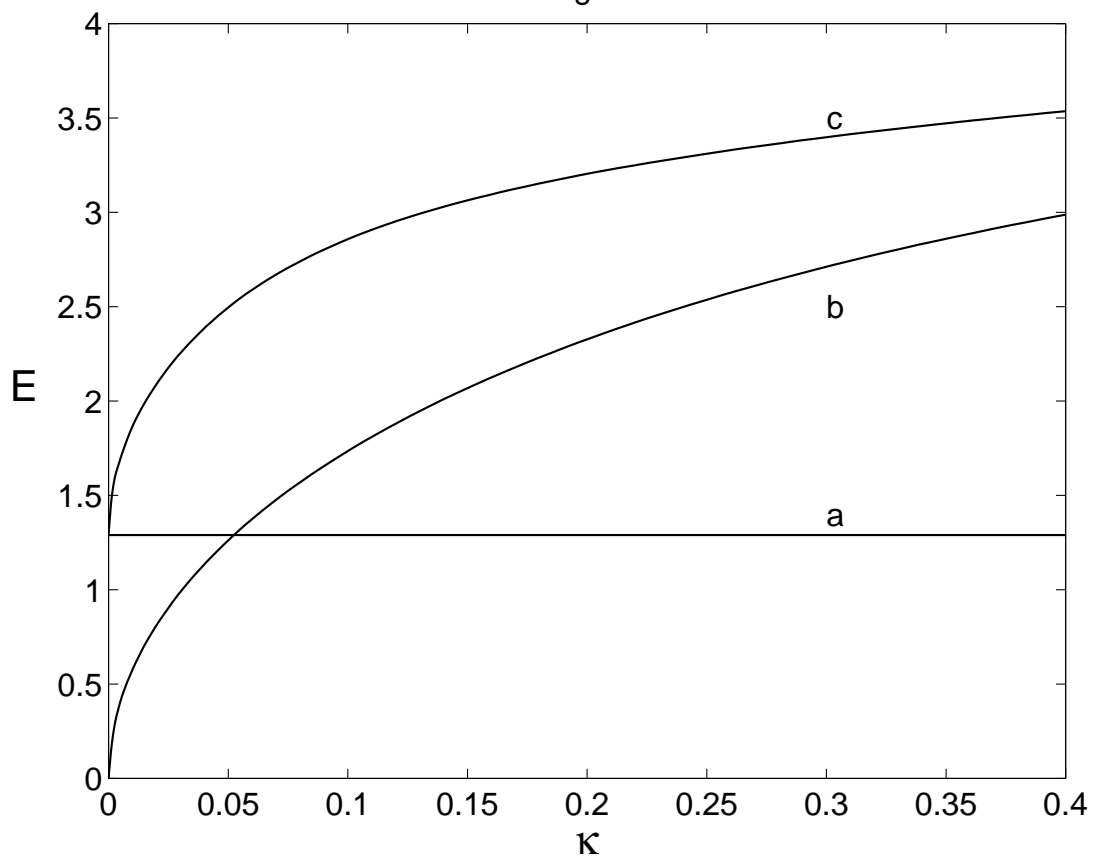


Fig. 2

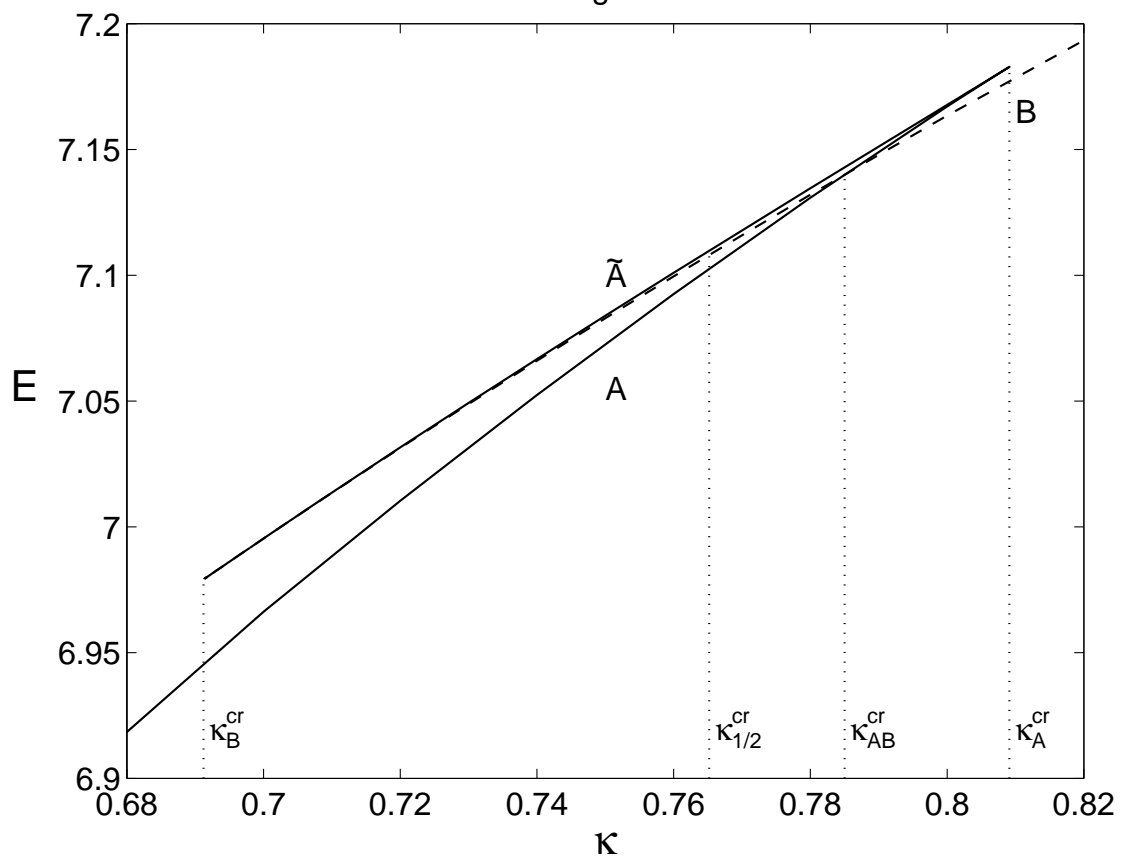


Fig. 3

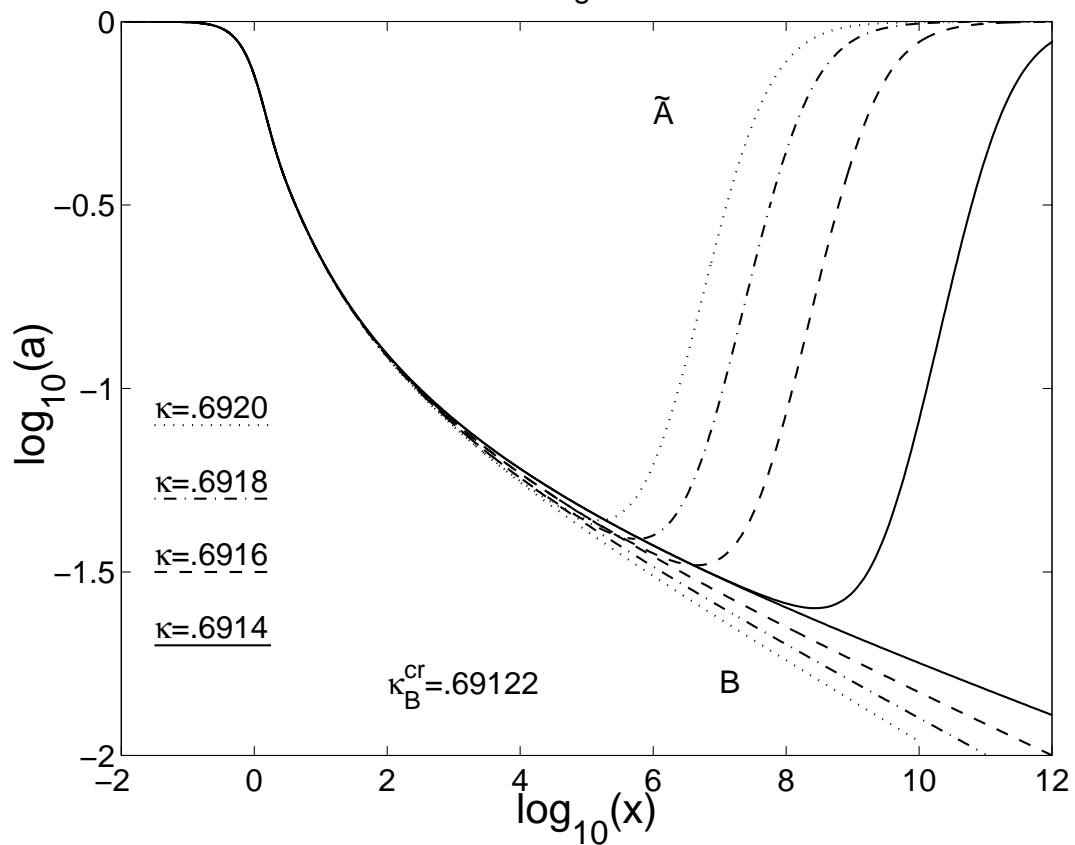


Fig. 4

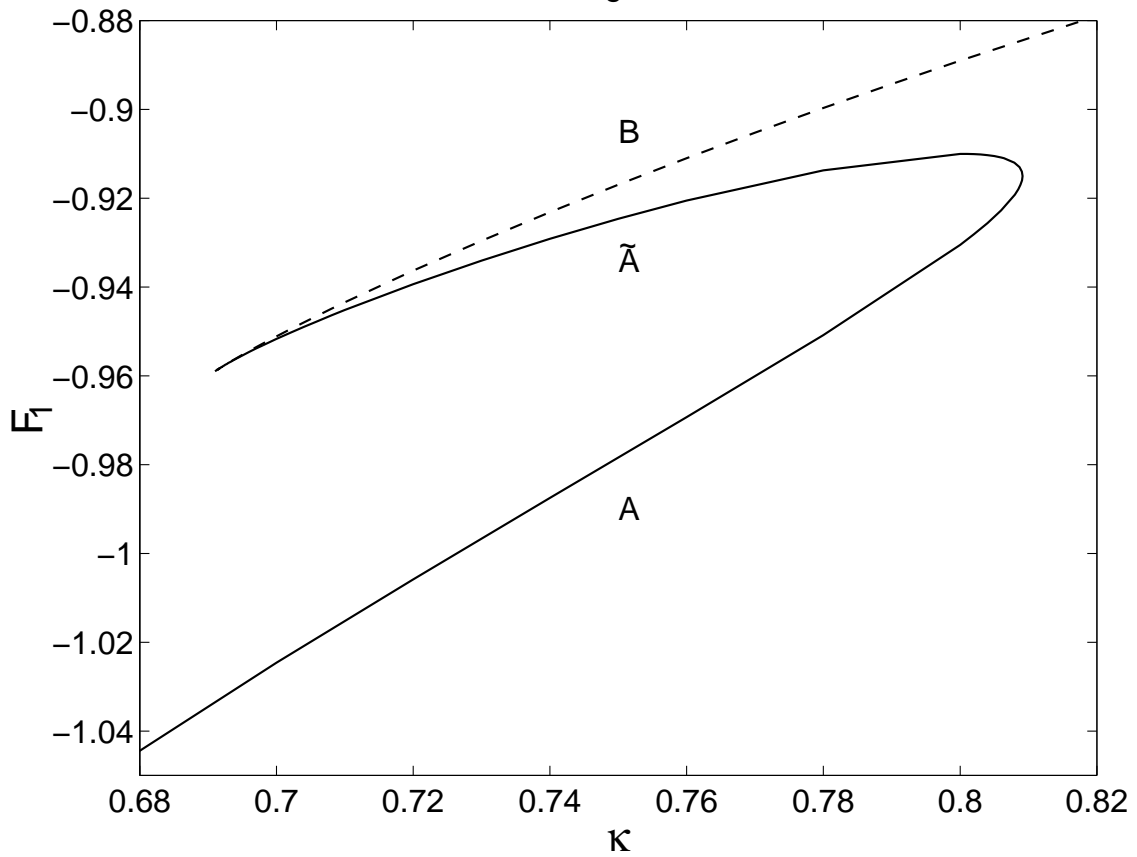


Fig. 5

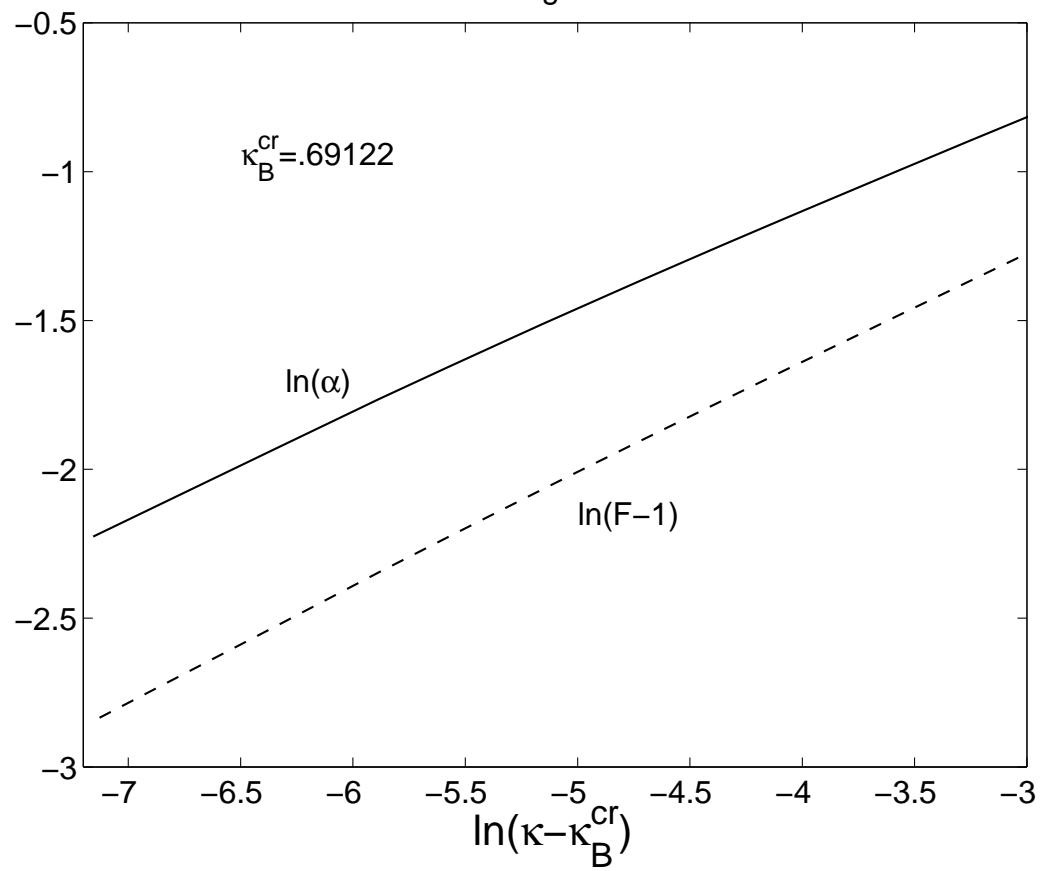


Fig. 6

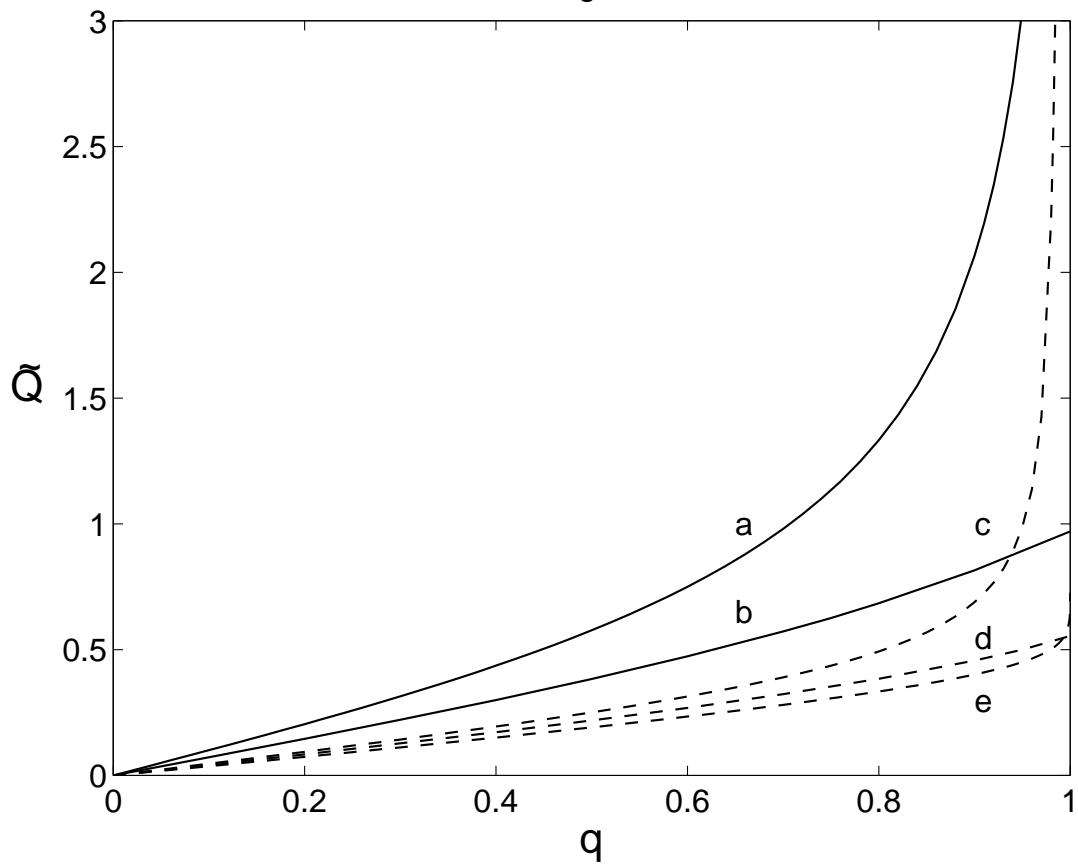


Fig. 7

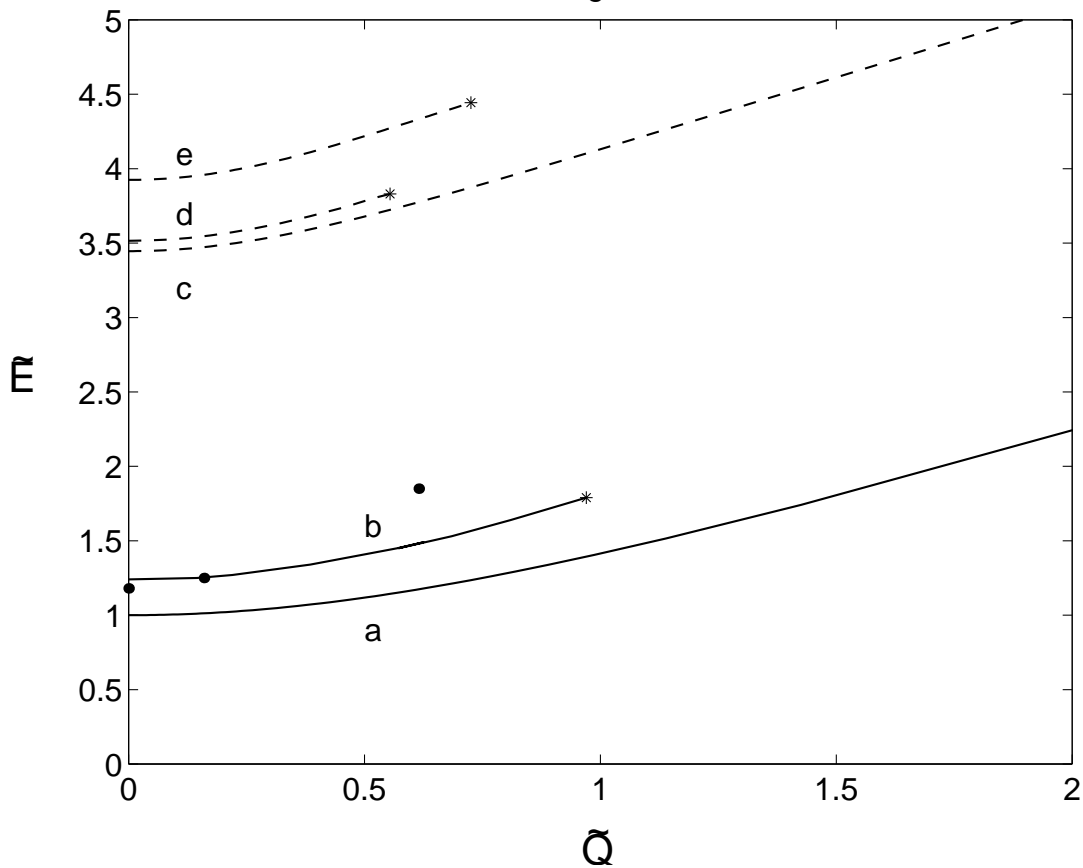


Fig. 8

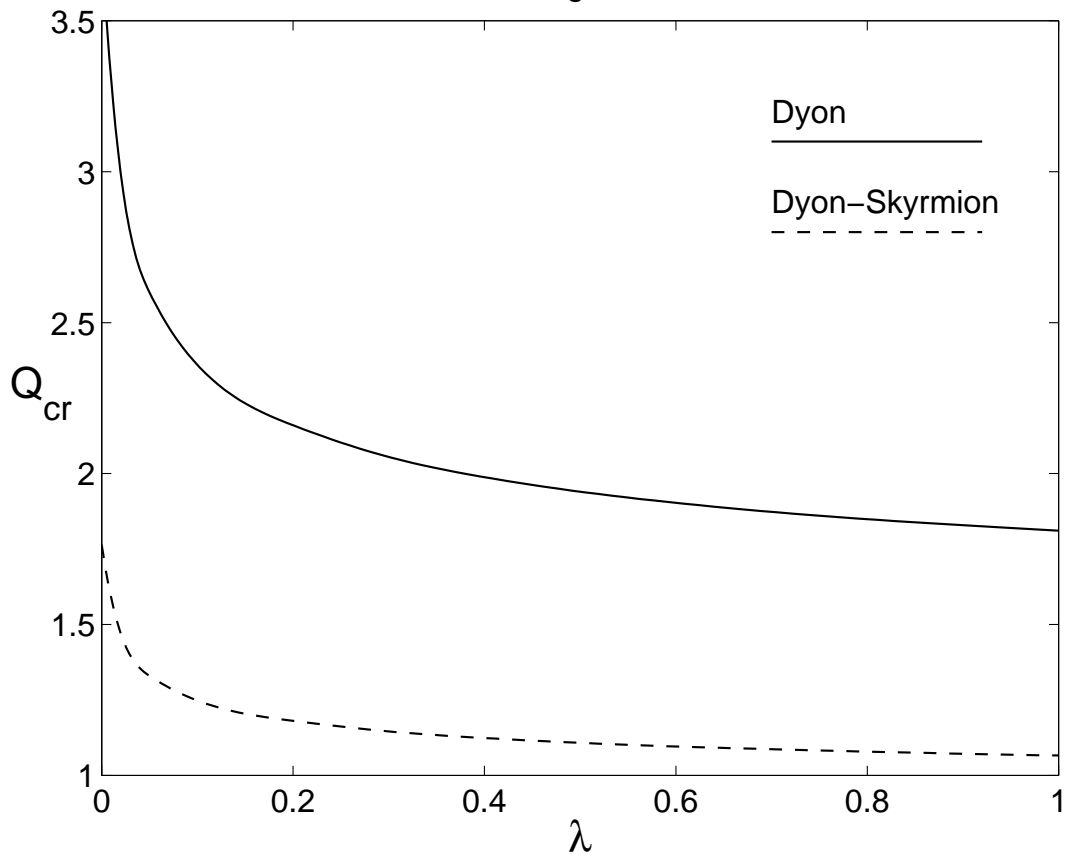


Fig. 9

